Formulation of subgrid stresses for large-scale fluid equations

Fernando O. Minotti and Sergio Dasso
Departamento de Física, Instituto de Física del Plasma, INFIP-CONICET, Universidad de Buenos Aires, 1428 Buenos Aires, Argentina
(Received 18 August 2000; revised manuscript received 25 October 2000; published 27 February 2001)

A formulation is presented based on a previously derived self-consistent procedure for obtaining subgrid scale models for complex system of equations. Using linear stability analysis and numerical simulations of the one-dimensional Burgers equation the formulation is shown to be very stable numerically and to reproduce accurately the large-scale flow of a high-resolution, direct simulation. Moreover, the resulting equation has a structure very similar to the viscous Camassa-Holm equation recently introduced in the modeling of turbulent flows.

DOI: 10.1103/PhysRevE.63.036306 PACS number(s): 47.27.Eq, 47.27.Ak

I. INTRODUCTION

Very recently [1] an approach was introduced to derive effective, large-scale equations for fluid systems directly from the dynamical equations. The large-scale equations differ from the original ones by the addition of new terms that arise due to the nonlinear character of the fundamental equations and represent the effect of small scales on the dynamic of the large-scale flow. These terms are generically termed subgrid scale terms (SGST). For quadratic or (integer) higher-order nonlinearities, common to fluid equations, the introduced formalism manages to express these SGST's as functions of only the large-scale flow, at the price of making some approximations, which can be quantified in terms of the nondimensional parameter ϵ, roughly the ratio of the smallest large scale resolved to the spatial scale of variation of the large-scale flow. The formalism is exact in the limit $\epsilon \to 0$, the error introduced being of order ϵ^3. When applied to the Navier-Stokes equations for an incompressible fluid the obtained SGST correspond to the differential version of the similarity model [2,3] which shows one of the highest correlations with real SGST in *a priori* tests [3]. The corresponding differential version is similar to that known in the literature as the gradient model [4,3] and shares with the self-similarity model a very high level of correlation in those tests (essentially equal), but happens to lead to strong instabilities in actual numerical simulations [5]. A possible remedy to ensure stability is to add a purely dissipative term of the Smagorinsky type [6] to the expression of the SGST or better still to limit the energy backscatter [3,7]. Although there exists a great deal of expertise in such an approach as applied to Navier-Stokes flows, in the spirit of deriving a formalism applicable to a variety of fluid systems, it is desirable to work out an expression that does not suffer from the above-mentioned instability.

The purpose of the present paper is to present a simple extension of the original formalism that preserves simplicity in the application to complex systems, and at the same time leads to much more stable equations. For the relative simplicity of the phenomenology involved and the possibility of analytical stability studies and well-controlled numerical simulations, we take Burgers equation as an example.

II. FORMALISM

In this section we briefly summarize the main results of the original formalism [1] as applied to a d-dimensional Burgers equation:

$$\frac{\partial \mathbf{v}}{\partial t} + (\mathbf{v}\cdot\boldsymbol{\nabla})\mathbf{v} = \nu \boldsymbol{\nabla}^2 \mathbf{v}, \tag{1}$$

where ν is the kinematic viscosity and $\mathbf{v}$ is the velocity field, a d-component vector function of the d-dimensional space coordinate $\mathbf{x}$ and of the time t.

The separation of scales in small and large is made with a filter, the top-hat filter, defined by the volume average

$$A(\mathbf{X},t) = \langle a(\mathbf{x},t)\rangle_{\mathbf{X}} = \frac{1}{\triangle V}\int a(\mathbf{x},t)\,dV, \tag{2}$$

where $\mathbf{X} = \langle \mathbf{x}\rangle_{\mathbf{X}}$ denotes the center of the d-volume $\triangle V$, and $a(\mathbf{x},t)$ is a generic field variable. Fluctuations of $a(\mathbf{x},t)$ around its average are defined as the difference

$$\delta a(\mathbf{X},\mathbf{x},t) = a(\mathbf{x},t) - A(\mathbf{X},t), \tag{3}$$

an approach originated by Schumann [8], which has the advantage of avoiding the generation of Leonard and cross terms [9,4]. In fact, definitions (2) and (3) lead to averages that satisfy Reynolds' postulates,

$$\langle A(\mathbf{X})\rangle_{\mathbf{X}} = A(\mathbf{X}), \quad \langle \delta a(\mathbf{X},\mathbf{x},t) A(\mathbf{X})\rangle_{\mathbf{X}} = 0, \tag{4}$$

which are valid with the fundamental proviso that the average should be performed around the same $\mathbf{X}$ on which all terms to be averaged depend. Moreover,

$$\left\langle \frac{\partial a}{\partial \mathbf{x}} \right\rangle_{\mathbf{X}} = \frac{\partial A}{\partial \mathbf{X}}. \tag{5}$$

Averaging of Eq. (1) is then very simple and leads to

$$\frac{\partial \mathbf{V}}{\partial t} + (\mathbf{V}\cdot\boldsymbol{\nabla}_{\mathbf{X}})\mathbf{V} = \nu \boldsymbol{\nabla}_{\mathbf{X}}^2 \mathbf{V} + \mathbf{S}, \tag{6}$$

where capital letters denote averages of the field represented by the corresponding lower-case letters, and spatial derivatives are all with respect to **X**. The last term corresponds to the SGST and is given by

$$\mathbf{S}(\mathbf{X}) = -\langle \delta\mathbf{v}(\mathbf{X},\mathbf{x}) \cdot \boldsymbol{\nabla}_{\mathbf{x}} \delta\mathbf{v}(\mathbf{X},\mathbf{x}) \rangle_{\mathbf{X}}. \tag{7}$$

The (approximate) expression of **S** can be obtained considering generic fields denoted by lower-case letters $a(\mathbf{x})$, $b(\mathbf{x})$, with top-hat average (2) about **X** represented by the corresponding upper-case letters $A(\mathbf{X})$, $B(\mathbf{X})$, and fluctuations (3) $\delta a(\mathbf{X},\mathbf{x})$, $\delta b(\mathbf{X},\mathbf{x})$. If the d volume $\triangle V$ is a d cube of side $\triangle$, and $\triangle V'$ is another d cube, also centered at **X**, but of side $2\triangle$, the following relations between averages in $\triangle V$ and $\triangle V'$ are easily obtained from Germano's identity [10,1]

$$A'(\mathbf{X}) = A(\mathbf{X}) + \frac{\triangle^2}{8} \boldsymbol{\nabla}_{\mathbf{X}}^2 A + O(\epsilon^4), \tag{8}$$

and

$$\begin{aligned} &\langle \delta a(\mathbf{X},\mathbf{x})\, \delta b(\mathbf{X},\mathbf{x}) \rangle'_{\mathbf{X}} \\ &= \langle \delta a(\mathbf{X},\mathbf{x})\, \delta b(\mathbf{X},\mathbf{x}) \rangle_{\mathbf{X}} + \frac{\triangle^2}{8} \boldsymbol{\nabla}_{\mathbf{X}}^2 \langle \delta a(\mathbf{X},\mathbf{x})\, \delta b(\mathbf{X},\mathbf{x}) \rangle_{\mathbf{X}} \\ &\quad + \frac{\triangle^2}{4} \boldsymbol{\nabla}_{\mathbf{X}} A \boldsymbol{\nabla}_{\mathbf{X}} B + O(\epsilon^4), \end{aligned} \tag{9}$$

where $\epsilon = \triangle / L_X$, with L_X the spatial scale of variation of averaged quantities, and where $O(\epsilon^4)$ represents the terms of order ϵ^4 and higher. For a generic relation of the form (9)

$$f' = f + \frac{\triangle^2}{8} \boldsymbol{\nabla}_{\mathbf{X}}^2 f + \triangle^2 q + O(\epsilon^4), \tag{10}$$

where f is the average of any fluctuating magnitude over $\triangle V$, f' the average of the same magnitude over $\triangle V'$, and q any expression independent of f containing averages over $\triangle V$, the general result is that f can be expressed as [1]

$$f = \frac{\triangle^2}{6} q + O(\epsilon^3). \tag{11}$$

For reference purposes we will denote relation (11) as model 0.

Use of Eqs. (4) and (5) shows immediately that, in Cartesian components, Eq. (7) can be written as

$$S_i = -\left\langle \delta v_j(\mathbf{X},\mathbf{x}) \frac{\partial \delta v_i(\mathbf{X},\mathbf{x})}{\partial x_j} \right\rangle_{\mathbf{X}}, \tag{12}$$

where summation of repeated indices is assumed. From Eqs. (11), (9), and (12) it then results

$$S_i = -\frac{\triangle^2}{24} \frac{\partial V_j}{\partial X_k} \frac{\partial^2 V_i}{\partial X_j \partial X_k} + O(\epsilon^3). \tag{13}$$

Equations (6) and (13) constitute a closed system for the large-scale field $\mathbf{V}(\mathbf{X},t)$ if the $O(\epsilon^3)$ are neglected. In what follows we will consider the one-dimensional version of this system, which can be written as

$$\frac{\partial V}{\partial t} + V \frac{\partial V}{\partial X} = \nu \frac{\partial^2 V}{\partial X^2} + \frac{\partial \tau}{\partial X}, \tag{14}$$

where the subgrid stress τ is expressed as

$$\tau = -\frac{\triangle^2}{48} \left(\frac{\partial V}{\partial X} \right)^2. \tag{15}$$

The system (14)–(15) will be denoted as Burgers model 0 (BM0). As neatly shown in Ref. [5], the nonviscous version of this equation is linearly unstable; in particular, severely unstable as, in a Fourier mode stability analysis, the growth rate of the instability increases rapidly with the number of Fourier modes taken into account.

III. EXTENDED FORMALISM

Consider Eq. (11) applied to f' in Eq. (10)

$$f' = \frac{\triangle'^2}{6} q' + O(\epsilon^3) = \frac{4\triangle^2}{6} q' + O(\epsilon^3). \tag{16}$$

Since q' is made up of magnitudes averaged over $\triangle V'$, denoted generically as A'_i, we can write

$$q'(A'_i) = q(A_i) + \sum \frac{\partial q}{\partial A_i} (A'_i - A_i) + O[(A'_i - A_i)^2].$$

Use of Eq. (8) to express $A'_i - A_i$ in terms of A_i leads to

$$\triangle^2 q' = \triangle^2 q + O(\epsilon^4),$$

which, together with Eq. (11), allows to write Eq. (16) as

$$f' = 4f + O(\epsilon^3). \tag{17}$$

This relation manifests the particular kind of fluctuations and averaging procedure employed. For instance, in the case of very smooth fields, the more usual definition of fluctuations $\delta a(\mathbf{x},t) = a(\mathbf{x},t) - A(\mathbf{x},t)$ leads to an f of order ϵ^4. Instead, fluctuations (3) lead to f proportional to $\triangle^2$, which verifies Eq. (17) for this special case.

When Eq. (17) is used in Eq. (10), it results

$$f - \frac{\triangle^2}{24} \boldsymbol{\nabla}_{\mathbf{X}}^2 f = \frac{\triangle^2}{3} q + O(\epsilon^3). \tag{18}$$

Equation (18) represents an alternative expression of the original model given by Eq. (11) that differs from the latter in terms of order ϵ^3; it will be denoted as model 1. It is interesting to mention here that both expressions, although rather different, give very similar SGST in the simulations performed in this paper, as it should be expected if terms of order ϵ^3 and higher remain small. However, expression (18) leads to much more stable equations than Eq. (11) as shown below.

With Eq. (18) the subgrid term **S** in Eq. (6) is now determined by

$$S_i - \frac{\triangle^2}{24}\nabla_{\mathbf{x}}^2 S_i = -\frac{\triangle^2}{12}\frac{\partial V_j}{\partial X_k}\frac{\partial^2 V_i}{\partial X_k \partial X_j} + O(\epsilon^3),$$

and the one-dimensional system expressed as

$$\frac{\partial V}{\partial t} + V\frac{\partial V}{\partial X} = \nu\frac{\partial^2 V}{\partial X^2} + \frac{\partial \tau}{\partial X}, \tag{19}$$

$$\tau - \frac{\triangle^2}{24}\frac{\partial^2 \tau}{\partial X^2} = -\frac{\triangle^2}{24}\left(\frac{\partial V}{\partial X}\right)^2, \tag{20}$$

which we call Burgers model 1 (BM1).

This system can be worked out to obtain an equivalent single equation for V:

$$\frac{\partial V}{\partial t} + V\frac{\partial V}{\partial X} = \nu\frac{\partial^2 V}{\partial X^2} + \frac{\triangle^2}{24}\left(\frac{\partial^3 V}{\partial t \partial X^2} + \frac{\partial V}{\partial X}\frac{\partial^2 V}{\partial X^2} + V\frac{\partial^3 V}{\partial X^3} - \nu\frac{\partial^4 V}{\partial X^4}\right), \tag{21}$$

which bears a strong similarity to the Camassa-Holm equation [11,12] if viscous terms are neglected and the identification of $\triangle^2/24$ with the α^2 appearing in Eq. (1) in Ref. [12] is made. Very recently, an n-dimensional, viscous version of the Camassa-Holm equation was proposed to model turbulent flow in channels and pipes with very good results [13,14]. In particular, the viscous terms in the viscous Camassa-Holm equation have exactly the same representation as in Eq. (21).

We now briefly consider the linear stability of the nonviscous version of system (19)–(20), essentially repeating the approach in Ref. [5]. For this we consider BM1 in a domain of length 2π, with periodic boundary conditions, with $\nu = 0$, and with a forcing term added to the right-hand side of Eq. (19) that is chosen so that $V(X,t) = \sin(X)$ is a stationary solution, with a corresponding τ whose explicit expression is not needed for what follows. Writing for small deviations from the stationary solution that

$$V(X,t) = \sin(X) + w(X,t),$$

$$w(X,t) = \sum_{k=-\infty}^{\infty} \omega_k(t)\, e^{ikX},$$

with an analogous decomposition for τ, the linearized system reduces to the infinite set of ordinary differential equations for $\omega_k(t)$

$$\frac{d\omega_k}{dt} = \frac{C\,k}{1 + C\,k^2}[(k+1)\omega_{k+1} + (k-1)\omega_{k-1}] + \frac{k}{2}(\omega_{k+1} - \omega_{k-1}), \tag{22}$$

where $C = \triangle^2/24$. Following Ref. [5] we replace this infinite system with a truncated one containing $N+1$ Fourier modes, that can be written in matrix notation as

$$\frac{d\mathbf{W}}{dt} = \mathbf{M}\mathbf{W},$$

where $\mathbf{W}$ is the column vector containing the $2N+1$ Fourier coefficients ω_k, and $\mathbf{M}$ is a $(2N+1)\times(2N+1)$ tridiagonal matrix with components easily deduced from Eq. (22). The problem is unstable if the maximum of the real part of the eigenvalues of $\mathbf{M}$ is positive. An upper bound for the real part of these eigenvalues can be easily determined from the coefficients of $\mathbf{M}$ as detailed in Ref. [5], given by

$$|\lambda_{\max}| \leqslant \frac{2C(N-1)^2}{1 + C(N-1)^2}. \tag{23}$$

We were not able to determine a lower bound, but expression (23) is enough for our purposes. A similar derivation applied to BM0 leads to

$$|\lambda_{\max}| \leqslant C(N-1)^2,$$

while a lower bound can be estimated, which has the same power-law behavior with N. The severeness of the instability is then apparent in the fast growth with N. This explosive behavior is suppressed by the Laplacian term in Eq. (20), which is responsible for the $C(N-1)^2$ term in the denominator of Eq. (23), thus ensuring that in the limit $N \to \infty$ the bound is finite. Linear instability is not excluded by our analysis, but in any case it is mild.

IV. NUMERICAL SIMULATIONS

To test the behavior of the different versions of the formalism under well-controlled conditions, we have solved numerically Eqs. (14) and (15) (BM0), and Eqs. (19) and (20) (BM1). The different results are compared to a fine resolution simulation of the one-dimensional version of Burgers equation (1), the solution of which is filtered with filter (2) to extract the large-scale fields. In all cases we have employed a fully spectral method in space, together with an Adam-Bashfort scheme of second order in time. Periodicity is imposed at the spatial boundaries of the region of length 2π. The fine resolution simulation evolves unforced from an initial condition of the form

$$v(x,t=0) = 4 + \cos(x) + \cos(5x) + \cos(10x) + \cos(15x) + \frac{1}{2}[\cos(64x) + \cos(512x)] \tag{24}$$

while the large-scale simulations start with the filtered version of Eq. (24). The viscosity is $\nu = 5\,10^{-3}$, the number of modes of the fine resolution simulation is 1024, and most of the large-scale simulations were performed with 64 modes, $\Delta = \pi/8$, and time step $\Delta t = 10^{-4}$. In principle, quite acceptable solutions can be obtained with as few as 256 and 16

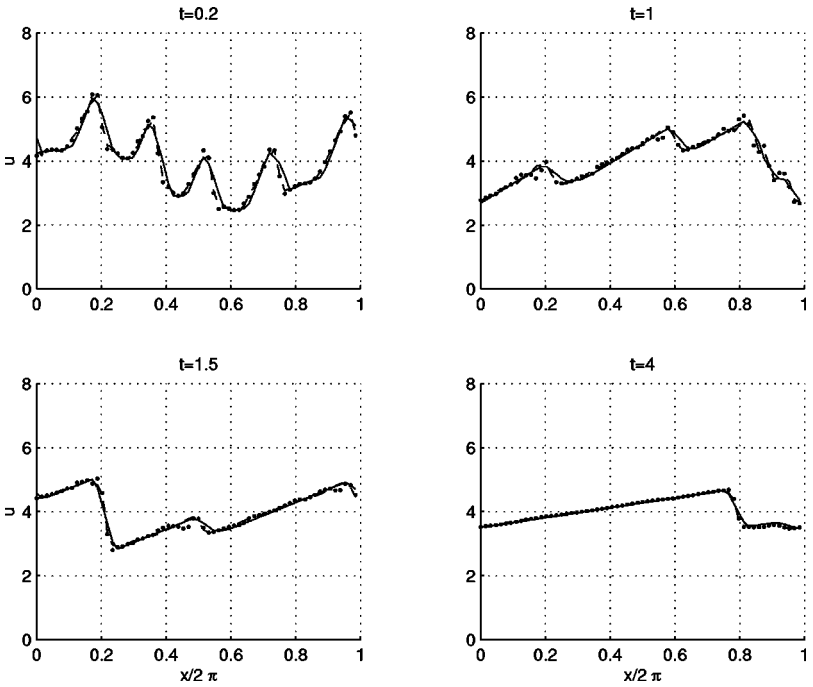

FIG. 1. Instantaneous profiles of large-scale velocity for time $t=0.2,1,1.5$, and 4. Solid line: average of the fine scale simulation. Dots: model BM0. Dashed line: model BM1. Units are arbitrary.

modes for the fine resolution and large-scale simulations, respectively, but we have kept the accuracy of the code high so that deviations from the exact solution are introduced by the large-scale models rather than by the numerical scheme.

Figure 1 shows the velocity profiles for fixed times $t=0.2$, 1, 1.5, and 4, obtained from the two large-scale simulations, BM0 and BM1, and from the filtered fine resolution simulation.

It is seen that the different solutions agree well, in particular, the shock positions in both large-scale simulations are essentially the same than in the filtered fine simulation as time evolves, indicating that no phase difference is introduced by the models. Model BM1 shows a smoother and more correct behavior than model BM0, that reflects itself in a better description of the smallest resolved scales of the flow, but not significantly in global quantities, as shown below.

Figure 2 shows the subgrid stresses of both models for the same times as in Fig. 1. It can be seen that the stresses are very similar, in spite of being defined by different expressions, even near the shocks where the subgrid stress and the higher order in ϵ terms neglected are more important.

Figure 3 shows the temporal behavior of the total energy for the three simulated cases. As can be seen, the decay of energy is very well represented by both models, with the scheme represented by BM1 a bit better than that represented

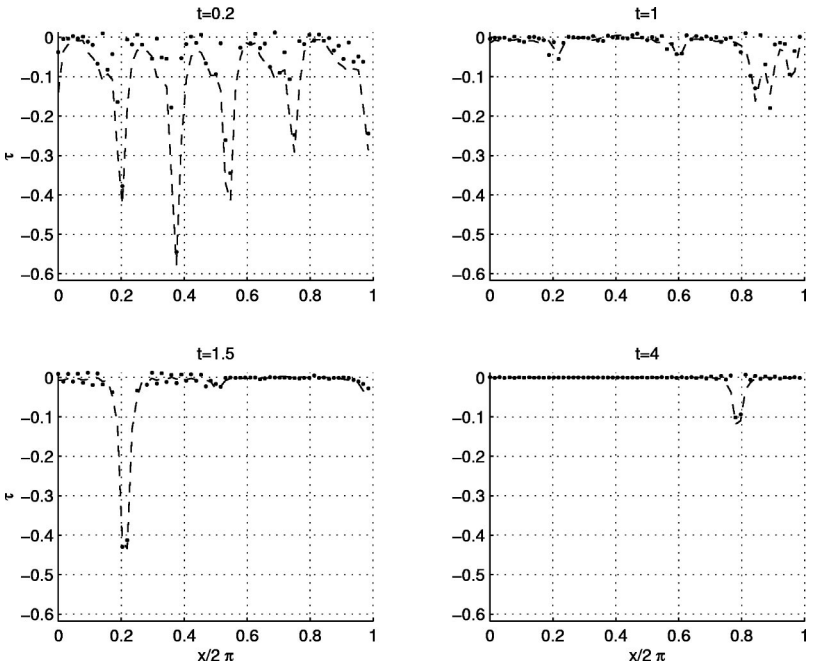

FIG. 2. Instantaneous profiles of subgrid stresses for time $t=0.2,1,1.5$, and 4. Dots: model BM0. Dashed line: model BM1. Units are arbitrary.

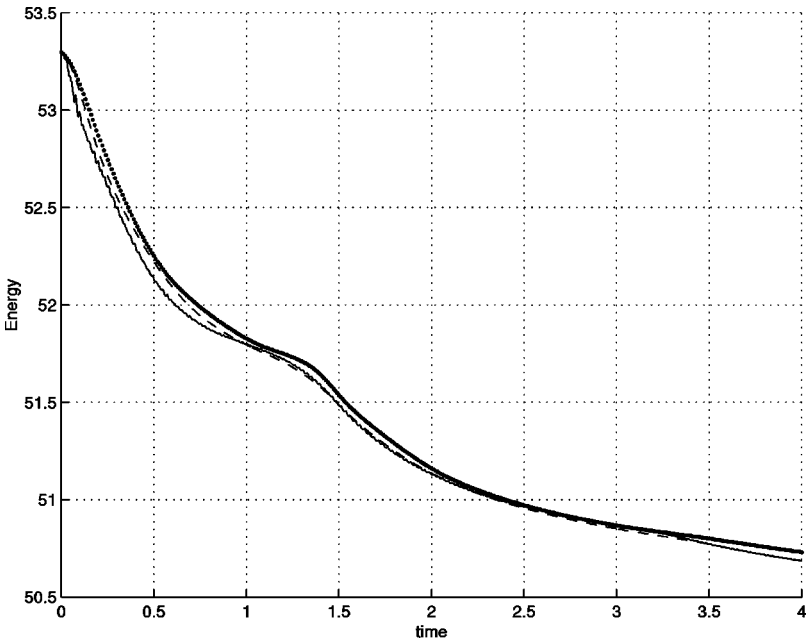

FIG. 3. Total energy as a function of time. Solid line: average of the fine scale simulation. Dots: model BM0. Dashed line: model BM1. Units are arbitrary.

by BM0. It is important to mention that most of the energy dissipation is due to the modeled SGST, as shown in Fig. 4. In this figure we display R, the ratio of total energy variation due to the SGST, to the total energy decay due to viscous dissipation, for both models BM0 and BM1. This ratio is given by

$$R = \int_0^{2\pi} V \frac{\partial \tau}{\partial X} dX \Big/ \int_0^{2\pi} \nu V \frac{\partial^2 V}{\partial X^2} dX,$$

which is positive when the subgrid stress globally extracts energy from the large-scale flow, a situation which we denominate as of direct cascade of kinetic energy. As can be seen in Fig. 4, there are two very noticeable negative peaks (each preceded by a strong positive peak) that indicate that at the corresponding instants a global inverse cascade of energy (backscatter) occurs. Of course, the model allows local backscatter to exist at any time, but the global backscatter turns out to exist only in very particular moments that we have identified with the merging of two shocks.

In order to emphasize the smallest resolved scales, we show in Fig. 5 a global quantity, which is proportional to what could be considered the enstrophy, defined as

$$\int_0^{2\pi} \left(\frac{\partial V}{\partial X} \right)^2 dX.$$

For these small scales the ratio ϵ has its largest value so that they are expected to be the worst described by the formalism. This is actually so; with large percent errors both large-scale

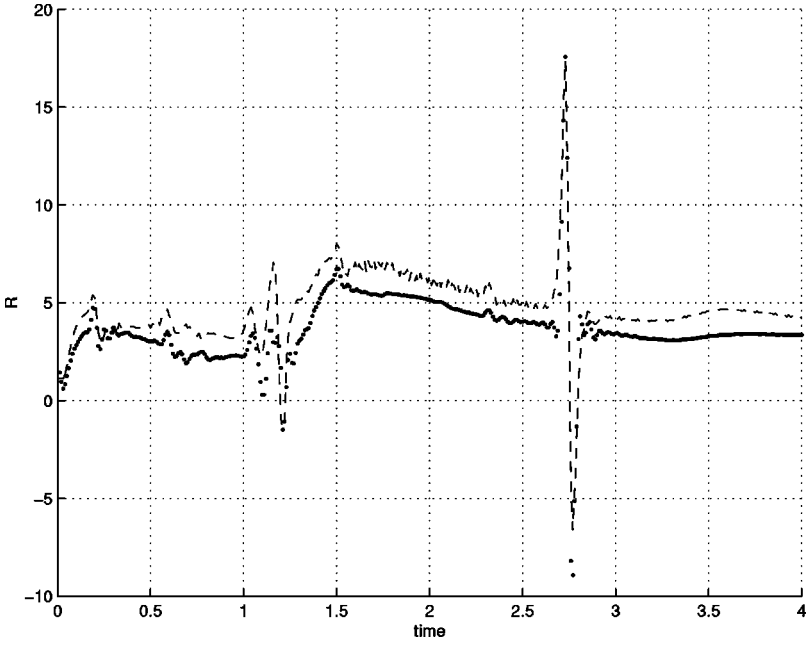

FIG. 4. Ratio of total-energy variation due to the subgrid stress, to the total-energy decay due to viscous dissipation, as a function of time. Dots: model BM0. Dashed line: model BM1.

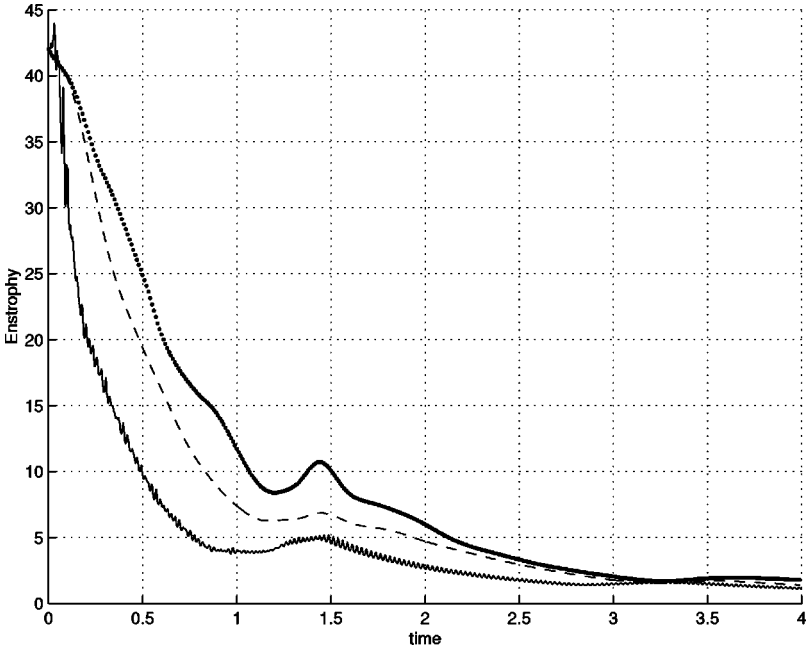

FIG. 5. Total enstrophy as a function of time. Solid line: filtered fine scale simulation. Dots: model BM0. Dashed line: model BM1. Units are arbitrary.

simulations follow the temporal behavior of the enstrophy of the filtered fine-scale velocity. BM1 is systematically closer than BM0 to the enstrophy of the ''exact'' case and reproduces better the different features; in particular, BM1 does not overestimate the hump occurring around $t=1.5$ as BM0 does.

An estimation of the error of the velocity in the large-scale simulations BM0 and BM1, represented by $V_0(X)$ and $V_1(X)$, respectively, is calculated as [expressing the filtered fine-scale simulation by $V(X)$]

$$E_{0,1}=\left(\frac{\int_0^{2\pi} [V_{0,1}(X)-V(X)]^2 dX}{\int_0^{2\pi} V^2(X)\, dX} \right)^{1/2} .$$

In Fig. 6(a) the error is shown for $\Delta=\pi/16$ and $\pi/8$ in model BM0, which turns out to be unstable for $\Delta=\pi/4$. Figure 6(b) shows the error for $\Delta=\pi/16$, $\pi/8$, and $\pi/4$ in model BM1. Not only is BM0 unstable for $\Delta=\pi/4$, but also its error is systematically larger than that of BM1, for corresponding values of Δ. The best choice is for both being $\Delta=\pi/8$, which corresponds to a Δ four times the smallest scale resolved by the numerical scheme.

Finally, we have solved Eq. (1) without any subgrid model using the same spatial resolution as in models BM0 and BM1, also starting from the average of Eq. (24). A instantaneous profile of the obtained velocity at time $t=1$ is shown in Fig. 7, along with the filtered fine resolution result and that of model BM1. As can be seen, a strong oscillatory behavior appears at small scales when no model is used,

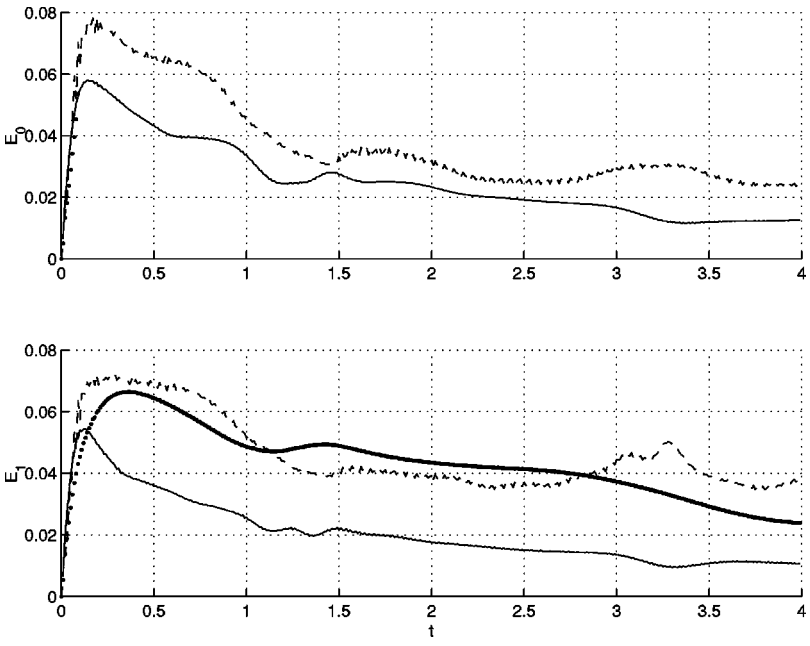

FIG. 6. Relative error of the large-scale velocity (see main text for a proper definition) as function of time, for different choices of filter length Δ. Solid line: $\Delta=\pi/8$. Dashed line: $\Delta=\pi/16$. Dots: $\Delta=\pi/4$. (a) Model BM0. (b) Model BM1.

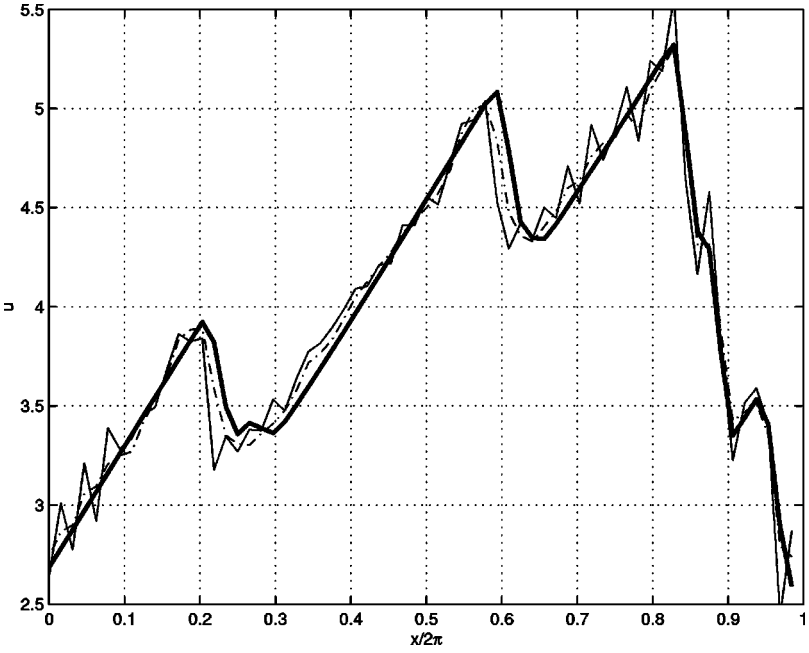

FIG. 7. Instantaneous profiles of large-scale velocity for time $t=1$. Thick-solid line: average of the fine scale simulation. Thin-solid line: low-resolution Burgers equation. Dashed-dot line: model BM1. Same units as in Fig. 1.

which is evidenced in the very large values of the enstrophy of this solution (not shown) which is at this time more than 8 times that of the ''exact'' value, while models BM0 and BM1 are, respectively, 2.7 and 1.7 times larger than the right value. This oscillatory behavior persists along the whole simulation, with corresponding large values of the enstrophy (more than 10 times the right values most of the time, while model BM1 never exceeds a factor of 2 over the correct solution).

V. CONCLUSIONS

We have presented an improved formulation of a previous model that preserves generality and is almost as simple but presents a much more stable behavior in numerical simulations than the original one. The new formulation also shows a systematically better performance for cases in which the original formulation is stable. Although the stability analysis and simulations were performed for the simple case of Burgers equation in one dimension, it is expected that more complex systems with similar nonlinear and diffusive behavior suffer from similar instabilities when the original formulation is used, and benefit from the alternative formulation as well. In principle, each fluid system requires a separate (in general difficult) study, the presentation in this paper being indicative of possible problems and solutions. From a more fundamental point of view, the numerical simulations have shown that both models reproduce well the large-scale flow (when the original formulation is stable), energy dissipation, etc., a behavior expected from the theoretical derivation of both models (they differ in terms of order ϵ^3) but not apparent due to the difference of their final expressions. Finally, it is remarkable that the new formulation leads to equations that are very similar to the viscous Camassa-Holm equation, considering that the respective derivations proceed along very different ways.

ACKNOWLEDGMENTS

This work was supported by the University of Buenos Aires (Grant UBACYT Ax38) and CONICET.

[1] F. O. Minotti, Phys. Rev. E **61**, 429 (2000).
[2] J. Bardina, J. H. Ferziger, and W. C. Reynolds, *Report TF-19*, Department of Mechanical Engineering, Stanford, 1984.
[3] S. Liu, C. Meneveau, and J. Katz, J. Fluid Mech. **275**, 83 (1994).
[4] R. A. Clark, J. H. Ferziger, and W. C. Reynolds, J. Fluid Mech. **91**, 1 (1979).
[5] B. Vreman, B. Geurts, and H. Kuerten, Theor. Comput. Fluid Dyn. **8**, 309 (1996).
[6] J. Smagorinsky, Mon. Weather Rev. **91**, 99 (1963).
[7] B. Vreman, B. Geurts, and H. Kuerten, J. Fluid Mech. **339**, 357 (1997).
[8] U. Schumann, J. Comp. Phys. **18**, 376 (1975).
[9] A. Leonard, Adv. Geophys. **18**, 237 (1973).
[10] M. Germano, J. Fluid Mech. **238**, 325 (1992).
[11] R. Camassa and D. D. Holm, Phys. Rev. Lett. **71**, 1661 (1993).
[12] D. D. Holm, J. E. Marsden, and T. S. Ratiu, Phys. Rev. Lett. **80**, 4173 (1998).
[13] S. Chen, C. Foias, D. D. Holm, E. Olson, E. S. Titi, and S. Wynne, Phys. Rev. Lett. **81**, 5338 (1998).
[14] S. Chen, C. Foias, D. D. Holm, E. Olson, E. S. Titi, and S. Wynne, Phys. Fluids **11**, 2343 (1999).